



ISTITUTO NAZIONALE DI RICERCA METROLOGICA Repository Istituzionale

An integrated approach to investigate climate-driven rockfall occurrence in high alpine slopes: the Bessanese glacial basin, Western Italian Alps

Original

An integrated approach to investigate climate-driven rockfall occurrence in high alpine slopes: the Bessanese glacial basin, Western Italian Alps / Viani, C; Chiarle, M; Paranunzio, R; Merlone, A; Musacchio, C; Coppa, G; Nigrelli, G. - In: JOURNAL OF MOUNTAIN SCIENCE. - ISSN 1672-6316. - 17:11(2020), pp. 2591-2610. [10.1007/s11629-020-6216-y]

Availability:

This version is available at: 11696/65194 since: 2021-01-27T10:49:31Z

Publisher:

SCIENCE PRESS

Published

DOI:10.1007/s11629-020-6216-y



Terms of use:


This article is made available under terms and conditions as specified in the corresponding bibliographic description in the repository


Publisher copyright


(Article begins on next page)


An integrated approach to investigate climate-driven rockfall occurrence in high alpine slopes: the Bessanese glacial basin, Western Italian Alps


VIANI Cristina^{1,2*}  <https://orcid.org/0000-0002-0993-0509>;  e-mail: cristina.viani@unito.it


CHIARLE Marta²  <https://orcid.org/0000-0001-8447-3822>; email: marta.chiarle@irpi.cnr.it

PARANUNZIO Roberta^{2,3}  <https://orcid.org/0000-0002-2270-7467>; e-mail: r.paranunzio@isac.cnr.it

MERLONE Andrea^{2,4}  <https://orcid.org/0000-0002-3651-4586>; email: a.merlone@inrim.it

MUSACCHIO Chiara⁴  <https://orcid.org/0000-0001-7473-3678>; e-mail: c.musacchio@inrim.it

COPPA Graziano⁴  <https://orcid.org/0000-0002-2847-3286>; e-mail: g.coppa@inrim.it

NIGRELLI Guido²  <https://orcid.org/0000-0002-5506-5915>; e-mail: guido.nigrelli@irpi.cnr.it

* Corresponding author

¹ Department of Earth Sciences, University of Torino, 10125 Torino, Italy

² Research Institute for Geo-Hydrological Protection, Italian National Research Council, 10135 Torino, Italy

³ Institute of Atmospheric Sciences and Climate, Italian National Research Council, 10133 Torino, Italy

⁴ National Institute of Metrological Research, 10135 Torino, Italy

Citation: Viani C, Chiarle M, Paranunzio R, et al. (2020) An integrated approach to investigate climate-driven rockfall occurrence in high alpine slopes: the Bessanese glacial basin, Western Italian Alps. *Journal of Mountain Science* 17(11). <https://doi.org/10.1007/s11629-020-6216-y>

© The Author(s) 2020.

Abstract: Rockfalls are one of the most common instability processes in high mountains. They represent a relevant issue, both for the risks they represent for (infra) structures and frequentation, and for their potential role as terrestrial indicators of climate change. This study aims to contribute to the growing topic of the relationship between climate change and slope instability at the basin scale. The selected study area is the Bessanese glacial basin (Western Italian Alps) which, since 2016, has been specifically equipped, monitored and investigated for this purpose. In order to provide a broader context for the interpretation of the recent rockfall events and associated climate conditions, a cross-temporal and

integrated approach has been adopted. For this purpose, geomorphological investigations (last 100 years), local climate (last 30 years) and near-surface rock/air temperatures analyses, have been carried out. First research outcomes show that rockfalls occurred in two different geomorphological positions: on rock slopes in permafrost condition, facing from NW to NE and/or along the glacier margins, on rock slopes uncovered by the ice in the last decades. Seasonal thaw of the active layer and/or glacier debuitressing can be deemed responsible for slope failure preparation. With regard to timing, almost all dated rock falls occurred in summer. For the July events, initiation may have been caused by a combination of rapid snow melt and enhanced seasonal thaw of the active layer due to anomalous high temperatures, and rainfall. August events are, instead, associated with a

Received: 19-May-2020

1st Revision: 14-Jul-2020

2nd Revision: 14-Aug-2020

Accepted: 14-Sep-2020

significant positive temperature anomaly on the quarterly scale, and they can be ascribed to the rapid and/or in depth thaw of the permafrost active layer. According to our findings, we can expect that in the Bessanese glacierized basin, as in similar high mountain areas, climate change will cause an increase of slope instability in the future. To fasten knowledge deepening, we highlight the need for a growth of a network of high elevation experimental sites at the basin scale, and the definition of shared methodological and measurement standards, that would allow a more rapid and effective comparison of data.

Keywords: Rockfalls; Climate change; Air and rock temperature; Periglacial environment; Western Italian Alps

Introduction

Rockfalls are one of the most common instability processes in high mountain slopes. They represent a relevant and topical issue, both for the risks they pose to high mountain structures, infrastructures, and frequentation (Ravanel et al. 2013; Macciotta et al. 2017; Mourey et al. 2019), and for their potential role as terrestrial indicators of climate change (Huggel et al. 2012; Paranunzio et al. 2016; Gallach et al. 2018; Hock et al. 2019).

For both aspects, it is crucial to assess the role of climatic parameters in the occurrence of rockfalls. Climatic parameters can act both as preparatory and triggering factors (Collins and Stock 2016; Di Matteo et al. 2017; McColl and Draebing, 2019; Pratt et al. 2019), while morpho-topographic and litho-stratigraphic settings influence the proneness of slopes to failure (Matasci et al. 2018).

The cryosphere has a key control on high elevation rock slope dynamics (Hasler et al. 2011; Haeberli and Whiteman 2015) through a variety of processes, often driven by phase changes of water (Draebing and Krautblatter 2019). For this reason, in high mountain, air temperature and rock temperature play a crucial role in slope dynamics: therefore, climate change, especially climate warming, is thought to have a significant impact on slope stability (Gariano and Guzzetti 2016; Patton et al. 2019).

Climate-related processes that can prepare mountain slopes for a slide act on timescales of years to millennia. In high mountains, rockfalls are an important consequence of paraglacial rock slope adjustment (Ballantyne 2002). A progressive rock strength degradation can result from: i) stress change in slopes and rock weathering following glacier recession (McColl and Davies 2012; Deline et al. 2015; Purdie et al. 2015; Vehling et al. 2016); ii) rock damage due to glacier fluctuations (Grämiger et al. 2018); iii) frost weathering (Thapa et al. 2017) and thermo-mechanical stresses due to temperature fluctuations, inducing crack opening or widening (Draebing and Krautblatter 2019); iv) permafrost degradation (Fischer et al. 2012; Krautblatter et al. 2013); v) diurnal and seasonal freeze/thaw cycles (Matsuoka et al. 1998; Regmi and Watanabe 2009; Nagai et al. 2013; Jia et al. 2015) and, more in general, cycles of thermal expansion/contraction (Collins and Stock 2016). Several studies have pointed out the crucial role of snow cover in controlling ground temperature and, consequently, thermal processes taking place in rock slopes (Haberkorn et al. 2015; Magnin et al. 2015; Draebing et al. 2017). Rock and debris moisture content also is crucial for the effectiveness of cryogenic processes (Sass 2005).

Climate-driven triggers act on timescales of hours to months. Rainfall events can cause a build-up of hydrostatic water pressure within rock fractures, and a consequent reduction of frictional strength: high intensity rainfalls are particularly effective in activating rockfalls (Krautblatter and Moser 2009; Matsuoka 2019). However, in high mountain, thermal processes appear to prevail in initiating rockfalls (McColl and Draebing 2019). In this regard, hydrostatic water pressure increase following rapid snowmelt in late spring and early summer (Stoffel et al. 2005; Draebing et al. 2014), and seasonal active-layer thaw in mid-summer and autumn (Gruber et al. 2004a) are noteworthy. When a clear trigger is missing, it is reasonable to assume that one or more of the aforementioned preparatory processes also acted as trigger (Kellerer-Pirklbauer et al. 2012; Phillips et al. 2017).

The growing interest for unrevealing the relationships between climate change and slope instability, driven by the increasing frequentation and use of high altitude territories (especially in the European Alps) and by the pace of climate change,

has led to an exponential growth of studies in the last 20 years. A formidable amount of observations, data, models, and hypotheses on climate-related processes leading to slope deformation and failure has been produced. Two main approaches are generally followed: i) the analytical study (through field monitoring, laboratory tests, modelling) of the physical processes contributing to rock deformation and/or weathering and worsening of rock-mechanical properties (e.g.; [Guglielmin et al. 2014](#); [Phillips et al. 2016](#); [Magnin et al. 2017](#); [Weber et al. 2017](#); [Mamot et al. 2018](#)); ii) a back analysis of the meteorological and climatic conditions associated with the occurrence of slope instability (e.g. [Allen and Huggel 2013](#); [D'Amato et al. 2016](#); [Nigrelli et al. 2018a](#); [Paranunzio et al. 2019](#); [Schlögel et al. 2020](#)).

Despite the remarkable efforts and the significant advances, uncertainties remain as to how climatic parameters control rockfall occurrence and therefore on the actual impacts of ongoing and expected climate change on rock slope instability ([Huggel et al. 2012](#)), in particular, considering the complexity of processes contributing to slope stability/instability and the interactions with the specific morpho-topographical and litho-structural conditions of the study areas ([Phillips et al. 2017](#); [Messenzehl et al. 2017](#); [Zangerl et al. 2019](#)). Specifically, the question remains whether the climate change has actually caused, and/or may in the future, an increase, or change, of rockfall hazard in high mountains, even though several evidences point in this direction ([Ravanel and Deline 2011](#); [Fischer et al. 2012](#)).

In order to deepen the knowledge on the relationship between climate change and natural instability processes that occur at high-elevation sites, monitoring activities and research carried out in climate observatories and high-elevation instrumented sites are thus crucial. In the Italian Alps, specific research is being carried out in the last decade in the framework of international projects, even if mostly focusing on monitoring of permafrost or individual slope instabilities ([Ravanel et al. 2018](#); [Mair et al. 2011](#)), or they are completed activities ([Occhiena et al. 2012](#)).

In this context, we aim to contribute to the growing topic of the nexus between climate change and slope instability at the basin scale. To our knowledge, the Bessanese glacial basin is to date

the only site in the Italian Alps which is specifically equipped, monitored and investigated for this purpose at the basin scale and not only at the scale of the single slope process.

For this purpose, in this paper we propose and discuss an integrated approach that combines geomorphological data with historical and instrumental ones. The method is also oriented toward establishing full data traceability and measurement uncertainty analysis, to promote more comparability with other and future works. This approach allows to analyze the high-resolution data collected in recent years (multiannual scale) on rockfall events, and on the associated climatic conditions and near-surface rock temperatures, in the broader context of local climate change (multidecadal scale) and of local, climate-driven, geomorphological dynamics (century scale).

1 Study Area

The study area is located in the Bessanese glacial basin (Graian Alps, North Western Italy; [Figure 1](#)). It has an extent of about 5 km², an elevation range from 2586 to 3620 m a.s.l., and corresponds to the hanging basin modelled by the local Pleistocene glacier.

The glacial basin is carved in the Oceanic Units of the Western and Ligurian Alps, especially in the Gastaldi Greenstones Zone. Calcschists and Metabasites are the prevailing lithotypes ([Piana et al. 2017](#)). Calcschists are found mainly in the eastern part of the study area, while Metabasites form the “Uja di Bessanese” ridge. In the southern part of the basin, an isolated outcrop of Serpentinites is found.

From a geomorphological point of view, the study area is overlooked by the “Uja di Bessanese” Peak (3620 m a.s.l.), with an up to 1000 m high rock wall that borders the glacial basin to the west. This rock wall, facing east-northeast, is cut by several incisions that channel block- and rock-falls, causing the formation of debris fans at the incisions’ outlet, in the southern part of the ridge. At the foot of the rock wall, the landscape is dominated by the Bessanese Glacier and by the neighbouring rock glacier named “Crot del Ciaussinet”. The huge left lateral moraine (length = about 770 m, max elevation = 2900 m a.s.l., min

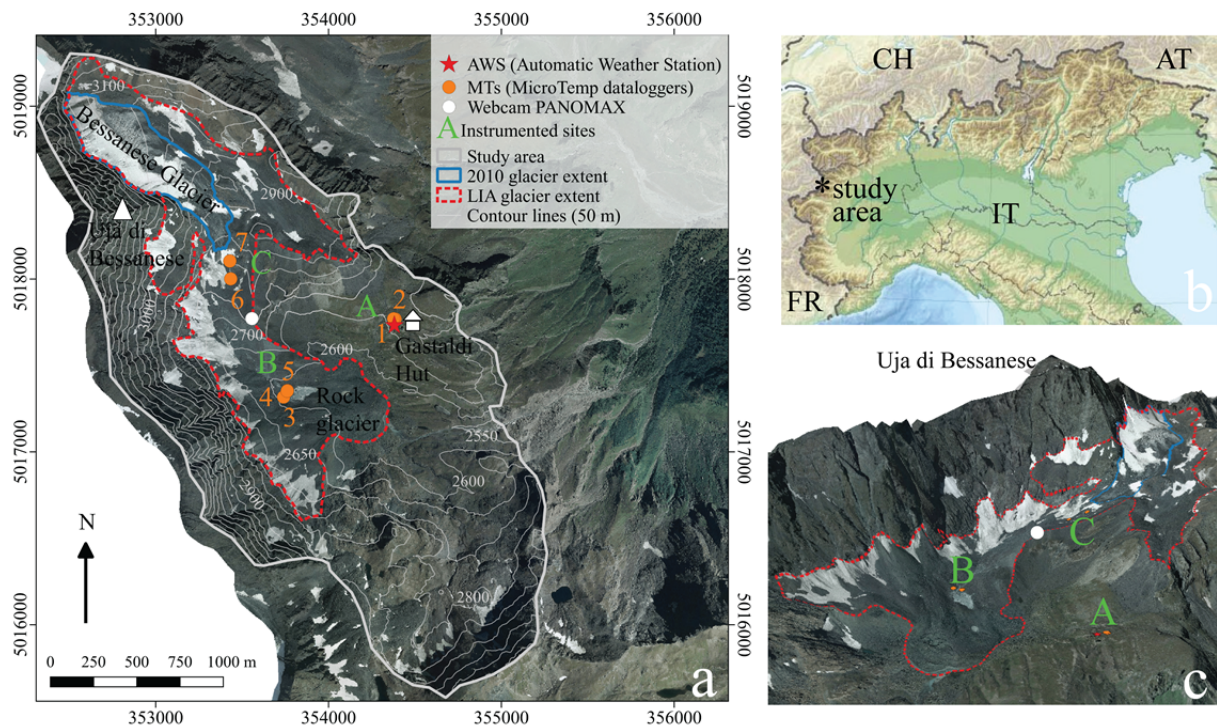


Figure 1 a) Outline of the study area with the location of the main geomorphological elements and places mentioned in the text (basemap 2010 orthophoto, reference system WGS84 / UTM 32N, source GEOportale Piemonte 2020); b) location of the study area with respect to northern Italy (IT = Italy, CH = Switzerland, FR = France, AT = Austria); c) 3D image of the study area (basemap 2010 orthophoto, source GEOportale Piemonte 2020).

elevation = 2600 m a.s.l.) formed by the western lobe of the Bessanese Glacier during the Little Ice Age (LIA) is a clear evidence of the dimensions attained at that time by the ice body. A smaller, eastern lobe of the glacier existed until the early 1990s (CGI 1996) and generated a debris accumulation north-west of the Gastaldi Hut. Since the end of the LIA (between 1845-1860 according to Orombelli 2011) the glacier shrunk mainly in its lowest, southern part, with a marked increase of the debris cover. The glacier area was about 1.75 km² at the LIA maximum (Lucchesi et al. 2014), it shrunk to 1.45 km² in the 1950s (CNR-CGI 1961) and in 2010 only 0.31 km² of ice remained (Smiraglia et al. 2015). Five lakes can be found in the proglacial area, changing in extent during time. According to the inventory by Viani et al. (2016), the largest lake (7265 m²) is located at 2581 m a.s.l. and was identified for the first time on the 2006 orthophotos.

According to Köppen's classification (Peel et al. 2007), the climate of the study area is "Polar". For the observation period 1989-2019, the mean annual air temperature is 0.4°C at 2659 m a.s.l. (data from the "Rifugio Gastaldi" Automatic

Weather Station, hereinafter AWS); the hottest month is August (mean temperature 8.1°C) and the coldest one is February (mean temperature -5.9°C).

The Alpine Permafrost Index Map (APIM; Boeckli et al. 2012), which classifies the likelihood of permafrost occurrence for the European Alps, indicates that permafrost in nearly all conditions can be found in the northern part of the study area including the northeast face of the "Uja di Bessanese" rockwall, and in the area nearby the Bessanese Glacier. The east face of the "Uja di Bessanese" rockwall, in the southern part of the study area, is characterized by variable permafrost conditions (i.e.: permafrost mostly in cold conditions and in nearly all conditions). Around the Gastaldi Hut and near the LIA glacial limit, permafrost is expected only in very favourable conditions. In order to verify the APIM indications, the Surface Frost Number (F+), an index of permafrost occurrence represented by the frost days (Barry and Gan 2011), has also been calculated, on a seasonal and annual basis. F+ is: 0.8 (winter), 0.6 (spring), 0.0 (summer), 0.4 (autumn) and 0.5 (Year), for the observation period 1989-2019. These values confirm the

presence of sporadic permafrost in correspondence to the AWS.

The Bessanese glacial basin has been chosen to become, since 2016, an open-air laboratory for studying the relationships between climate forcing and geomorphological dynamics, especially slope instabilities, in a context of climate warming. This choice was due to the variety of geomorphological elements and processes that can be found in this relatively small area. Moreover, a high altitude AWS with a 30-year record is available, and a strategic structure for the logistics and for communication and dissemination purposes, the Gastaldi Hut, is present. This open-air laboratory is ideal for collecting data, developing and testing new methodological approaches, and comparing different tools and technologies, with an interdisciplinary imprint.

2 Materials and Methods

A cross-temporal and integrated approach has been adopted for this study (Figure 2). Geomorphological investigations, covering a multidecadal/century time interval, and an analysis of the local climate (last 30 years) have been carried out. The objective is to provide a broader context for the interpretation of the high-resolution data collected in recent years in the

Bessanese experimental basin on rockfall events, climatic conditions associated to their occurrence, and near-surface rock temperatures.

Geology has not been specifically considered in this study, since it controls location, type and size of instability processes, rather than their timing and frequency (Fischer et al. 2012), which are the main focus here.

2.1 Geomorphological analysis

The geomorphological analysis has been aimed to the identification of: i) past rockfall occurrences, their timing, location and characteristics of source and accumulation areas; ii) the main geomorphological elements of the study area and of their evolution at the multidecadal/century scale, with a focus on glacier thickness change, as a preparatory factor of slope instability (Deline et al. 2015).

2.1.1 Rockfall events identification

In order to retrieve rockfall events occurred in the study area, the following sources have been considered: i) reports of the annual CGI glaciological surveys (CGI 2020): 52 annual reports are available for the study area, covering the period 1928-2018 with some interruptions, especially during the 1940s and the 1980s; ii) multitemporal aerial photos and orthophotos: orthophotos

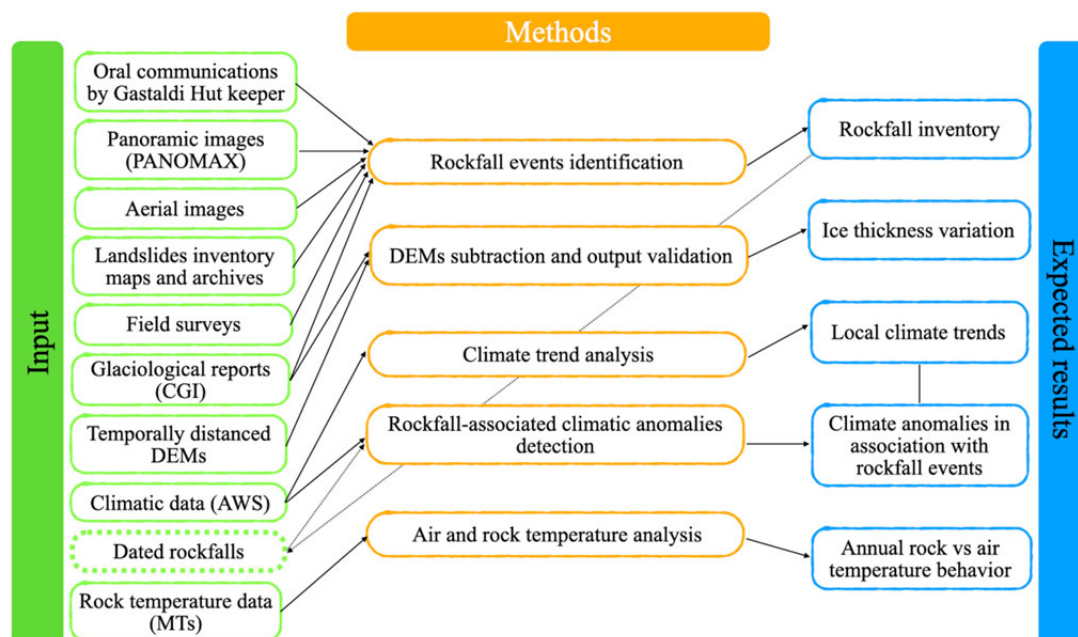


Figure 2 Workflow of the cross-temporal approach adopted in this study.

relating to 6 different times in the period 1988–2012 are available on the Italian National Geoportal, aerial photos relating to 5 different times in the period 1954–2004 have been taken by the Italian Military Geographic Institute, and aerial photos relating to 18 different times in the period 1945–2009 can be viewed on the French National Geoportal; iii) landslide inventories: the [IFFI \(2020\)](#) and [SIFRaP \(2017\)](#), respectively the national and regional landslide inventories, have been consulted; iv) historical archives of IRPI-CNR; v) news on the web. Since 2016, with the start of activities in the Bessanese experimental basin, direct information has come from the reports of the Gastaldi Hut keeper, from field investigations and from 360° webcam images (see Section 2.3).

2.1.2 Estimate of the Bessanese Glacier thickness change

Two digital elevation models (DEMs) are available for the study area, made approximately 20 years apart. The oldest one was acquired in the 1985–1994 period and has a resolution of 50 m and a vertical uncertainty of ± 10 m, while the most recent one was derived from a LiDAR aerophotogrammetric flight realized in the period 2009–2011 and has a resolution of 5 m and a vertical uncertainty of ± 0.60 m ([Belotti et al. 2013](#)). The comparison, in a GIS environment, of the two DEMs allowed to assess elevation changes occurred in the study area and, specifically, to estimate the change in surface elevation of the Bessanese Glacier, with an uncertainty of about ± 10 m, due to DEMs vertical uncertainty ([Wang and Kääb 2015](#)).

The reports of the annual CGI glaciological surveys ([CGI 2020](#)) allowed to validate elevation change data resulting from the difference of DEMs. In fact, starting from the 1990s, Franco Rogliardo, the local operator of CGI, has been measuring the annual elevation change of the Bessanese Glacier surface at two benchmarks. One reference mark is located in the lower part of the accumulation zone of the glacier, on a rock outcrop at 2950 m a.s.l. A second benchmark is located at 2877 m a.s.l., where the western lobe of the glacier heads south, confined by the imposing LIA lateral moraine.

2.2 Climatic analyses

Local climatic analyses have been carried out

to: i) characterize the study area and identify climate trends; ii) detect eventual climatic anomalies associated with rockfall occurrences.

The climatic data used for this purpose come from the “Rifugio Gastaldi” AWS (owner ARPA Piemonte). The AWS is located at 2659 m a.s.l. and is active since 1988. The AWS measures air temperature, relative humidity, wind speed and direction, rainfall amounts, snow depth (since 1990), total incident and reflected solar radiation (since 2018).

Daily minimum, maximum and mean air temperature data acquired by the AWS were used for climatic trend analysis on monthly, seasonal, and annual basis (observation period 1989–2019). For this purpose, the non-parametric Mann-Kendall test was used, by means of dedicated software ([Štěpánek 2006](#)). The Mann-Kendall test is a rank-based, non-parametric test for verifying trend significance and is largely used to assess the significance of trends in hydro-meteorological time series. The advantage of this test is that it is distribution-free and does not assume any special form for the distribution function of the data, including censored and missing data ([Sneyers 1990](#); [Nigrelli et al. 2015](#)).

Trend analyses were performed on the following parameters: mean (Tmean), maximum (Tmax) and minimum (Tmin) air temperature, extreme minimum (extreme Tmin) and maximum (extreme Tmax) air temperature. Trend analyses were also carried out on the following parameters, defined according to [WMO \(2009\)](#) indications: number of frost-free (FFD, $T_{min} > 0^{\circ}\text{C}$), frost (FD, $T_{min} \leq 0^{\circ}\text{C}$), icing (ID, $T_{max} \leq 0^{\circ}\text{C}$) days.

Precisely dated rockfall events have been investigated from a climate perspective by applying the statistical-based method described in [Paranunzio et al. \(2019\)](#). The method is based on an empirical distribution function to determine whether one or more climate variables V have assumed anomalous values prior to the occurrence of a slope failure event. The cumulative probability $P(V)$ has been estimated in a non-parametric way as $P(V) = i/n+1$, if $V > V_{(i)}$. The variable V is assumed to be a significant triggering factor at the α level when $P(V) \leq \alpha/2$ (negative anomaly) or $P(V) \geq 1 - \alpha/2$ (positive anomaly). The significance level α is set to 0.2, thus a 10% test on each of the distribution tails is performed. In the end, the

variable V is assumed to be a significant factor for the preparation/initiation of rockfalls when $P(V) \leq 0.1$ or $P(V) \geq 0.9$. This approach aims to catch an eventual climate signal in the triggering and/or preparation of a slope failure by detecting anomalous values in the climate variables (temperature and precipitation) associated with the occurrence of the considered events.

2.3 On-site monitoring and data analysis

A set of temperature data loggers has been installed in the study area in order to acquire data on the thermal conditions of the rocks. They have been compared with the air temperature data, for a deeper understanding of the relationships between thermal conditions and development of geomorphological processes, with particular attention to slope instabilities. A webcam was also installed, for visual monitoring of the study area, aimed at documenting the environmental conditions (weather conditions, snow cover, local sunrise and sunset, etc.) associated with rock temperature records, and the possible occurrence of rockfalls.

2.3.1 Instrumentation

The miniaturized temperature data loggers installed in the Bessanese experimental basin to monitor near-surface rock temperature (NSRT) are the MadgeTech MicroTemps (hereinafter MTs). These sensors have been selected for the purposes of this study since they are equipped with replaceable batteries, they offer easy download, robustness and waterproof, together with appropriate resolution and data storage capabilities. By replacing the batteries, the thermometers can be calibrated several times, before and after the measurement period, establishing measurements traceability to SI standards. It is possible to use

them for several years, by accessing the site in summer, downloading data, bringing them to the calibration laboratory, making a new “fresh” calibration, and bringing them in place again. This improves the data quality and its comparability in time and space.

The MTs have been metrologically validated before installation: a dedicated procedure was defined as one of the activities of the MeteoMet project (Merlone et al. 2018), in order to a) adopt a dedicated calibration procedure, able to better represent the measurement conditions met by the sensors in field and b) provide an evaluation of the measurement uncertainty (not limited to the calibration uncertainty, but including the field effects), by testing batches of sensors in field and minimizing the uncertainty contributions through a relative approach. The overall measurement uncertainty turned out to be $\pm 0.1^\circ\text{C}$ (Merlone et al. 2015; Nigrelli et al. 2018b). Data acquisition has been set every 30 min, in order to obtain datasets easily comparable with the AWS ones, which consist of data recorded every 10 min. For this study, MTs were installed at 10 cm depth in rock, in 3 locations with different lithological and morpho-topographic characteristics (Figure 1a and Table 1): A) a Calcschists rock outcrop near the Gastaldi Hut and the AWS; B) two Metabasites boulders in proximity of the main proglacial lake; C) an outcrop of Metabasites with Calcschists intercalations, close to the active front of the Bessanese Glacier. The horizontal distance between MTs and AWS ranges between 40 m and 700 m, while the maximum difference in elevation is about 130 m: AWS data can thus be considered representative of weather conditions at the instrumented sites. Data series used for this study (stored in the Pangaea repository; Nigrelli et al. 2018c) ended in 2018, because from this year onwards the sensors have been moved to other

Table 1 Main characteristics of the rock faces where the MTs were positioned. Site: A = Gastaldi Hut, B = close to the main proglacial lake, C = below glacier front. Lithology: CS = Calcschists, MCSI = Metabasites with Calcschists intercalations, M = Metabasites.

MTs	Site	Location	Geology	Elevation (m a.s.l.)	Aspect (°)	Slope (°)	Data series (ddmmyyyy)
1	A	Outcrop	CS	2667	250	30	20072016-16072018
2	A	Outcrop	CS	2666	36	85	20072016-16072018
3	B	Boulder	M	2594	90	30	20072016-15082018
4	B	Boulder	M	2586	53	80	20072016-15082018
5	B	Boulder	M	2586	234	80	20072016-15082018
6	C	Outcrop	MCSI	2772	180	80	17082017-15082018
7	C	Outcrop	MCSI	2790	125	80	17082017-15082018

locations in the same experimental basin, to carry out different, still ongoing, experiments.

Parallel to the installation of the MTs, a webcam has been placed on the left lateral LIA moraine of the Bessanese Glacier, at an elevation of 2775 m a.s.l. (<https://bessanese.panomax.com/>). This special webcam is particularly suitable for the purposes of this study because it acquires images with a high resolution, allowing excellent enlargements; at the same time, thanks to the particular scanning technique, images are not very heavy and therefore particularly suitable for transmission even in difficult environmental conditions. The webcam captures images with time intervals ranging from 10 to 30 min, with a 360° view, allowing the monitoring of most of the study area. These images are archived in a special repository and can be easily consulted remotely at any time by everybody, even after several years.

2.3.2 Data Analysis

Several parameters have been derived from NSRT datasets: i) the mean annual surface temperature (MAST); ii) the annual variability (including minimum and maximum temperature and the annual range); iii) the maximum diurnal range; iv) the number of effective freeze-thaw cycles (EFTCs), defined by Matsuoka (1990) as a fall below -2°C of the rock temperature followed by a rise above $+2^{\circ}\text{C}$.

The same analysis has been carried out on air temperature and successively compared with the results obtained from the NSRT.

The images acquired by the webcam have been checked on a daily basis, to detect the possible occurrence of slope instabilities. Moreover,

webcam images have been fundamental to establish the different types of weather, to verify the presence/absence of snow and of solar irradiation conditions in the measurement sites during the MTs acquisition periods.

3 Results

3.1 Rockfall activity in the study area

Ten main rockfall events located in the study area have been identified (Table 2, dots in Figure 3 show the detachment zones). The earliest documented event dates back to 1956 (CGI 1959) and produced a “large” rockfall deposit on the glacier front, located at that time upstream of the glacial lake at 2581 m a.s.l. The second one, reported in 1958 (CGI 1961), was described as a “recurring fall of blocks” from the incisions in the Bessanese rockwall. The information provided by the reports of the glaciological surveys is not sufficient to exactly define the spatial location and occurrence time of these events, which, nevertheless, testify the proneness to rockfall of the Bessanese NE facing rockwall. No further notice of rockfall occurrence was found in the various data sources until the early 1990s. The comparison among multitemporal aerial photo datasets on the Italian and French geoportals allowed to identify a rockfall accumulation with large blocks that occurred in the period 1990–1994 from the S facing slope of the Punta Adami ridge, to the northern border of the study area (Figure 4): this is the only event documented in this sector and its volume can be estimated in some thousands m^3 . In the hot

Table 2 List of the rockfalls identified by the present study with indication (where available) of the date of the event and the characteristics of the detachment zone (description, lithotype, elevation, slope, aspect).

Date	Detachment zone				
	Description	Lithotype	Elevation (m a.s.l.)	Slope (°)	Aspect
1956	Cuts in the Bessanese rock wall	Metabasites	above 2800	40–70	NE
1958	Cuts in the Bessanese rock wall	Metabasites	above 2800	40–70	NE
1990–1994	S slope of Punta Adami	Metabasites	3091	49	188
2003	NE ridge of the Uja di Bessanese	Metabasites	2996	28	73
End of Sep. 2016	Cuts in the Bessanese rock wall	Metabasites	above 2800	40–70	NE
2017-08-27	NE ridge of the Uja di Bessanese	Metabasites	2996	28	73
2018-08-30	Next to Punta Rosenkrantz	Metabasites	above 2800	40–70	NE
2019-07-06	NW face of Cresta del Fort	Calchschiefs	2906	50	334
2019-07-17	NE ridge of the Uja di Bessanese	Metabasites	2996	28	73
2019-08-23	NE face from Rocca Affinau	Serpentinities	2800	40	25
	Below LIA left lobe limit	Metabasites	2700–2900		
	Below LIA left lobe limit	Metabasites	2700–2900		
	Below LIA left lobe limit	Metabasites	2700–2900		

summer 2003, on occasion of the annual glaciological survey (Armando et al. 2004), a rockfall was reported, which originated from the base of the NE ridge of the Uja di Bessanese and deposited on the western lobe of the glacier at about 3000 m a.s.l. More in general, the report

describes the summer 2003 as a period of enhanced rockfall activity in the Bessanese glacial basin. The six most recent events were reported by the Gastaldi Hut keeper, as a result of the active collaboration started within the project of the Bessanese experimental site. At the end of

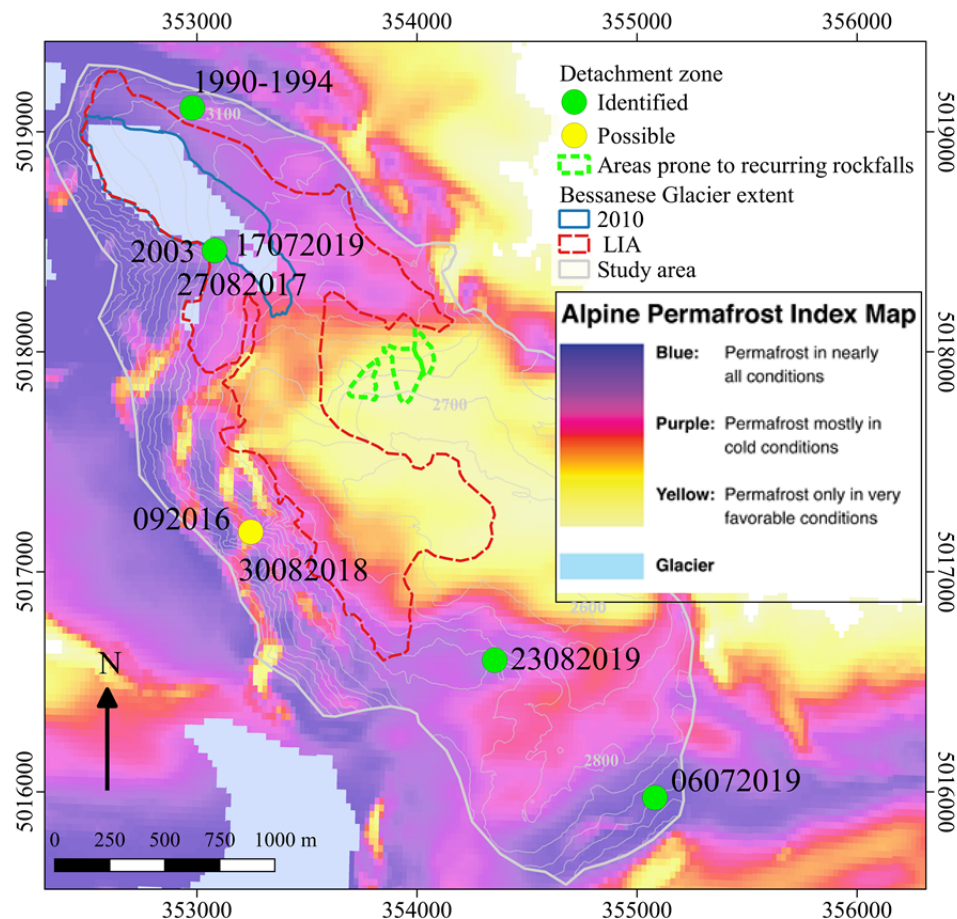


Figure 3 Map illustrating the location of the rockfall events identified by the present study (Basemap APIM, reference system WGS84 / UTM 32N, source: <https://geoserver.geo.uzh.ch/cryogis/wms>, University of Zurich).

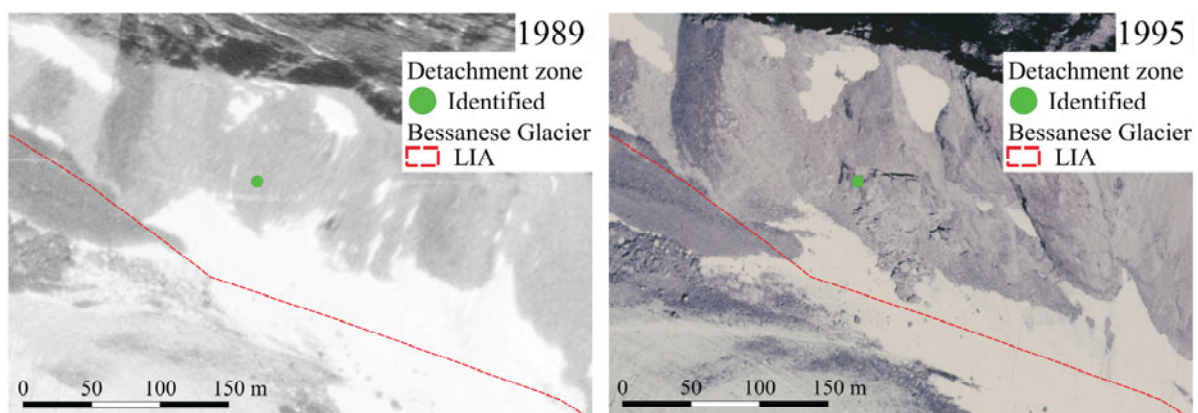


Figure 4 Comparison between two orthophotos before (a, 1989; source Italian National Geoportal) and after (b, 1995; source French Géoportail) the rockfall event dated 1990-1994 from the S facing slope of the Punta Adami ridge (reference system WGS84 / UTM 32N).

September 2016, a rockfall detached from one of the cuts in the Bessanese rock wall and generated a well visible cloud of dust. On August 27, 2017 at 10:55 (CEST), a rock mass collapsed from the NE ridge of the Uja di Bessanese and deposited on the surface of the Bessanese Glacier, about 250 m upstream of the glacier front. Probably the largest event documented in the study area occurred on July 6, 2019 at 16:00 (CEST), when a large (several thousands m³) rock mass detached from the NW face of “Cresta del Fort”: the foot of the slope was still covered with snow and thus the accumulation was clearly identifiable. On July 17, 2019 at 23:00 (CEST) a rock spur detached from the base of the NE ridge of the Uja di Bessanese, about in the same location where the 2003 and 2017 events occurred: the rockfall produced a loud noise, which lasted several minutes, and was heard distinctly at the Gastaldi Hut. On August 23, 2019 at 12:51 (CEST) a rockfall detached from the top of the NE rockwall of Rocca Affinau. A cloud of dust is clearly visible on the photos taken by the Gastaldi Hut keeper. The volume of the collapsed mass must have been small, since a survey carried out a few days later did not allow to clearly identifying the detachment and accumulation areas. In addition, the report of the glaciological campaign carried out on August

29-30, 2018 (Baroni et al. 2019) mentions “signs of instability in the rock cut next to Punta Rosenkrantz (the same where the September 2016 rockfall occurred), with small, sporadic falls of rock”.

Finally, on the landslide inventory maps of the IFFI and SIFRaP projects, three areas defined as “prone to recurring rockfalls” have been identified: these areas are located immediately below the LIA limit of the eastern lobe of the Bessanese Glacier, but no information is available about their timing (green dotted lines in Figure 3). Searches on the web and in the historical archives of the CNR-IRPI and the analysis of the webcam images did not provide information on additional instability events.

3.2 Ice thickness variation of the Bessanese Glacier

In recent decades, the Bessanese Glacier suffered a substantial mass loss (Figure 5a and 5b). Thanks to two temporally distanced DEMs it was possible to quantify the elevation change of the glacier surface with an uncertainty of ± 10 m (Figure 5c). The mean surface elevation lowering can be estimated in about 20 m in the period

1990s-2011. The highest ice losses occurred in the lowest part of the western lobe, where the glacier surface lowered of about 35 m, and in most of the accumulation area, where the surface elevation change was about 20-30 m. On the contrary, losses in the order of 10-20 m are found along the western margin of the accumulation area of the glacier, likely because of snow avalanche feeding from the Bessanese NE face. Even lower values can be found in the portion of the glacier located immediately below the 2010 front limit: this area is steeper than the rest of

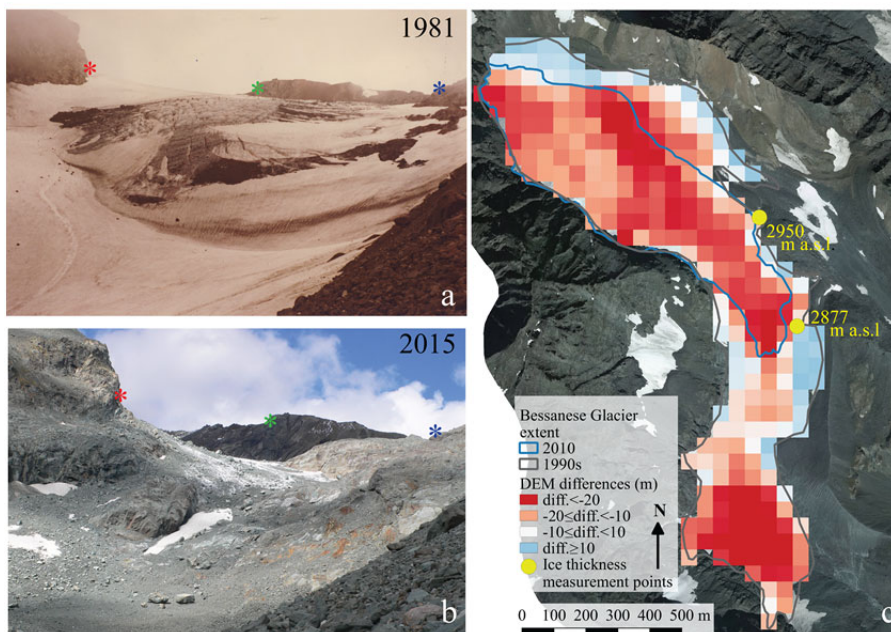


Figure 5 a) Bessanese Glacier in 1981 (photo D. Marangoni, CGI archive); b) Bessanese Glacier in 2015 (photo M. Chiarle): the asterisks * indicate the corresponding points in the two photos; c) glacier areal and surface elevation changes in the period 1990s-2010 (basemap 2010 orthophoto, reference system WGS84 / UTM 32N, source GEOportale Piemonte 2020).

the glacier, and thus ice here was presumably thin (Linsbauer et al. 2012; Viani et al. 2020) and rapidly thawed away, causing the 1990s glacier tongue to separate from the accumulation area in the years 2000s. For the period 1991-2011, the cumulative glacier thickness changes measured by the CGI operator at two benchmarks located at 2950 and 2877 m a.s.l. (yellow dots in Figure 5c), were respectively -12 m and -28 m, in good agreement with the results of DEM subtraction. In the following years (2012-2018) additional ice losses of about 4 m and 9 m were reported, respectively, at the higher and lower benchmarks. Based on a photographic comparison, the CGI operator estimated, for the period 1900-1990, a lowering of the glacier surface of about 25-30 m.

The mass loss of the Bessanese Glacier is similar to that of another glacier of comparable size, elevation and exposure located in the Graian Alps and monitored since the beginning of the 1990s: the Ciardoney Glacier lost about 24 m in the 1992-2010 time period (Nimbus 2015). In summary, the lowering of the surface of the Bessanese Glacier since 1900 can be estimated in about 30-60 m, depending on the considered glacial sector. The lowering rate more than doubled from 1990 onwards, from 0.3 m/y in the period 1900-1990 to 0.6 m/y since 1991 at the highest benchmark, and to 1.4 m/y at the lowest one. These data are in perfect agreement with the WGMS data that account for a loss of ice mass for monitored glaciers in the European Alps in-between 0.4 meters water equivalent per year (m w.e./y) and 1.4 m w.e./y for the period 1997-2017 (<https://climate.copernicus.eu/glaciers-o>).

3.3 Local climatic trends

Trend analysis applied to some climatic parameters is reported in Table 3 (obs. period 1989-2019).

This analysis confirms, also for the study area, a clear warming trend. Significant trends ($p < 0.05$) have been found for all the considered parameters in summer and for the majority of parameters in autumn; on the contrary, few and less significant trends have been identified in spring and only one in winter (number of frost days, FD). On an annual basis, temperature showed significant warming trends in four of the five air temperature

Table 3 Seasonal and annual trend (obs. period 1989-2019) of some climatic parameters (Mann-Kendall trend test, significance 95%, see §2.2). Mean (Tmean), maximum (Tmax) and minimum (Tmin) air temperature, extreme minimum (ETmin) and extreme maximum (ETmax) air temperature ($^{\circ}\text{C}/10$ years). Number of frost-free days (FFD), frost days (FD), icing days (ID) (days/10 years). Dashes indicate no significant trend. Winter: December-January-February; Spring: March-April-May; Summer: June-July-August; Autumn: September-October-November.

Parameters	Win.	Spr.	Sum.	Aut.	Year
Tmean	-	-	0.7	0.6	0.4
Tmax	-	0.8	0.8	0.8	0.6
Tmin	-	-	0.6	0.6	0.4
ETmin	-	-	0.9	-	-
ETmax	-	0.9	0.8	0.6	0.7
FFD	-	-	5	5.2	13.2
FD	-0.8	-	-5	-5	-12.1
ID	-	-3.8	-1	-	-

parameters, especially in the maximum temperature ($+0.6^{\circ}\text{C}/10$ years) and its extreme values ($+0.7^{\circ}\text{C}/10$ years). These findings are in line with trends detected in North-Western Italian Alps by previous studies (e.g., Acquafredda et al. 2015). Moreover, a general increase has been recorded in the number of frost-free days, FFD ($+5.0$, $+5.2$ and $+13.2$ days/10 years in summer, autumn and in the annual aggregation respectively). In parallel, the number of frost days (FD) decreased in summer (-5.0 days/10 years), in autumn (-5.0 days/10 years) and annually (-12.1 days/10 years). The number of icing days (ID) dropped only in spring (-3.8 days/10 years) and in summer (-1.0 days/10 years).

3.4 Climate anomalies for dated rockfalls

A statistical investigation of the contingent climate conditions for the sole precisely located and dated rockfalls (August 27, 2017, July 6 and 17, and August 23, 2019) has been conducted according to Paranunzio et al. (2019) (Figure 6). The analysis has revealed that all the considered events are associated with a positive temperature anomaly (i.e., above 90th percentile) at daily, weekly and quarterly scale on almost all considered parameters, with a prevalence in mean and minimum air temperatures. More specifically, just considering those variables that turned out to be significant (28%), it has been found that respectively 32% and 35% of anomalies are ascribable to mean and minimum air temperatures.

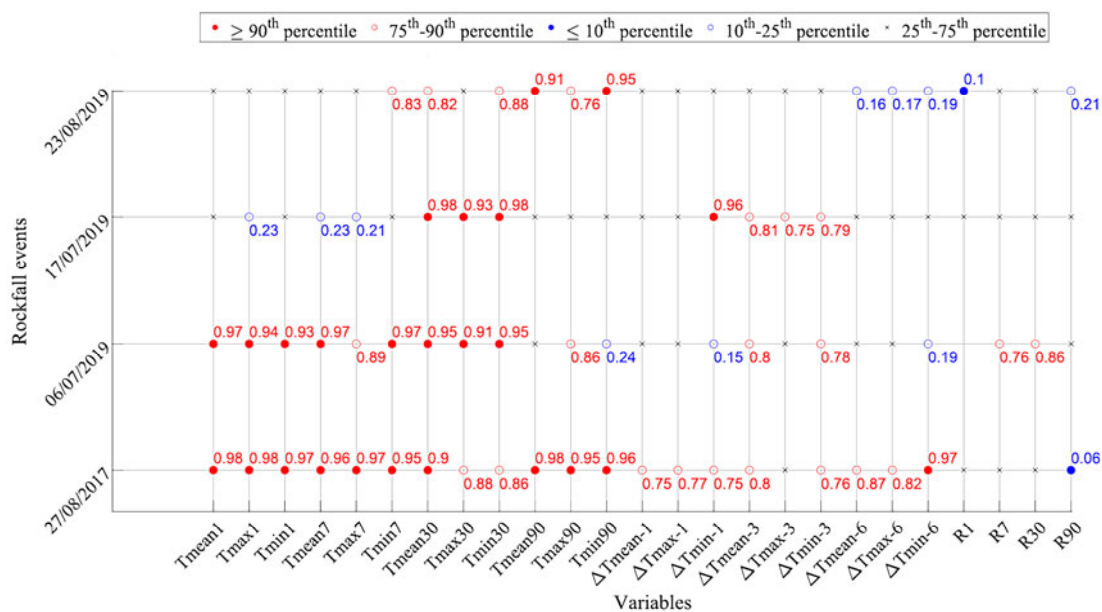


Figure 6 Estimation of the non-exceedance probability $P(V)$ estimation according to [Paranunzio et al. \(2019\)](#) associated with the variable V , being V : temperature (T), precipitation (R) or temperature variation between the day of the failure and the days before (ΔT). The aggregation range is reported; i.e. daily range (1), weekly range (7), monthly range (30), and quarterly range (90) for T and R , while ΔT refers to the previous day (-1), 3 days (-3), and 6 days (-6) before failure. Mean, max and min refer to mean, maximum and minimum average temperatures. Significant positive anomalies are filled red, whereas significant cold anomalies are filled blue. Percentiles below 25th and above 75th are indicated. No symbol has been used when no precipitation was recorded. For precipitation, probability values below 50th percentile, meaning few and/or not abundant precipitation with values below the median value, are not of interest.

The two events occurred at the end of August share a clear positive temperature anomaly at the quarterly scale. On the other hand, the two events occurred in July 2019 share a pronounced positive temperature anomaly at the monthly scale.

Based on our analysis, precipitation values do not show relevant anomalies except in the July 2019 events, for which non-exceedance probability values turned out to be above the median in some cases. More in detail, precipitation associated to July 6 event is above 75th percentile at weekly and monthly scale and, on July 17 event, values are over 65th percentile at the weekly scale. In this regard, it should be recalled that, since the rain gauge is not heated, undercatch bias when precipitation is in solid form (as in spring) could occur. Thus, precipitation might in some cases be underestimated (e.g., precipitation at the quarterly scale for July events).

3.5 Annual rock and air temperature behaviour

NSRTs vary inter-annually but in parallel in

the three sites and show a clear link with air temperature fluctuations from July to November. In winter and spring, instead, because of the snow cover, rock temperature remains close to 0°C for long periods: in winter, the snow cover insulates the ground from air temperature below 0°C (zero curtain), preventing its cooling; in spring, latent heat consumption due to snowmelt process relatively cools the ground, thus impeding ground heating ([Zhang et al. 2005](#)). An example of annual NSRTs variation is shown in [Figure 7](#).

MAST was always positive but there was a drop from the first to the second measurement period ([Table 4](#)): MAST ranged from 2.5°C to 3.9°C in 2016-17, and from 0.3°C to 2.8°C in 2017-18. Also MAAT was positive in both periods and was higher in 2016-2017 (1.8°C), than in 2017-2018 (0.7°C). Compared to air temperature, rock temperatures were always higher in their minimum and maximum annual values. MAST was higher than MAAT in the 2016-2017 period for all MTs, but lower than MAAT in the subsequent period for the two MTs facing NE (n. 2 and 4). The latter MTs also show, for both measurement periods, lower

Table 4 Mean Annual Air Temperature (MAAT), Mean Annual Surface Temperature (MAST), annual range and diurnal maximum ranges of air (AWS) and near-surface rock temperature from 1 August 2016 to 31 July 2017 (first period) and from 1 August 2017 (from 17 August 2017 for MT 6 and 7) to 31 July 2018 (second period). All data are in degrees Celsius; nd, no data.

MTs	2016-2017					2017-2018				
	MAAT/ MAST	Annual fluctuation			Max diurnal range	MAAT/ MAST	Annual fluctuation			Max diurnal range
AWS	1.8	Min	Max	Annual range		0.7	Min	Max	Annual range	
1	3.5	-22.1	21.0	43.1	21.0	1.0	-25.8	18.0	43.8	17.5
2	2.8	-10.1	35.4	45.5	26.4	0.3	-14.7	32.3	47.0	24.4
3	2.8	-10.4	30.0	40.4	19.6	0.3	-15.7	23.2	38.9	16.8
4	3.9	-5.9	38.7	44.6	29.0	2.8	-13.1	39.4	52.5	29.0
5	2.5	-10.1	26.6	36.7	17.6	0.1	-13.9	26.9	40.9	14.0
6	2.8	-5.8	31.4	37.2	23.7	0.5	-13.0	33.1	46.2	18.5
7	nd	nd	nd	nd	nd	1.7	-6.5	28.7	35.1	21.3
	nd	nd	nd	nd	nd	0.9	-13.1	25.1	38.2	18.0

annual and maximum diurnal ranges, compared to AWS. Considering annual fluctuation, the highest maximum temperature recorded was 39°C at MT 3 (facing E) in 2017-2018, which is also the sensor with the largest annual range. Considering diurnal ranges, the largest one was again recorded at MT 3 in both periods, with a measured value of about 29°C.

From September to November, MTs experienced several effective freeze-thaw cycles (Table 5). EFTCs varied from a minimum of 4 to a maximum of 12 cycles in the first period (Sept.-Nov. 2016) and from 1 to 15 cycles in the second period (Sept.-Nov. 2017). In general, the number of EFTCs in the air was higher than in the rock, with the exception of MTs 3 and 4 in October 2016, and of MT 7 in November 2017. Considering sites A and B, in 2017 the period characterized by freeze-thaw cycles started comparatively earlier (14/09/2017) with respect to 2016 (09/10/2016). The number of EFTCs was similar for site A in both years but at site B it was higher in 2016 compared to 2017. The highest number of EFTCs was recorded at site C in 2017, mainly in November. After the period dominated by EFTCs, in 2016, at sites A and B, a progressive cooling to sub-freezing conditions occurred until the beginning of November while, in 2017, this transition lasted until the end of December in all three sites. Successively, winter cooling was followed by seven (2016-17) or eight (2017-18) months of stable thermal conditions, between 0°C and 2°C (zero curtain periods), with no diurnal oscillation in snow covered sites. In late spring or beginning of summer, temperatures rise to positive values, concluding the annual freeze-thaw cycle started in winter before the snow cover onset.

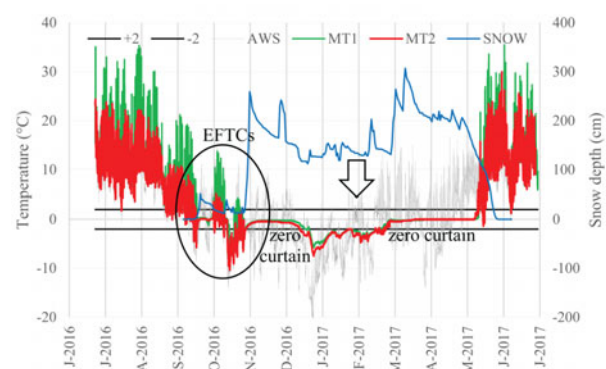


Figure 7 Rock and air temperatures during the 2016-2017 period at the Gastaldi Hut instrumented site. Periods of EFTCs in the rock are underlined by the black ovals and the $-2^{\circ}\text{C} < t < +2^{\circ}\text{C}$ thresholds are represented by the two black horizontal lines. The black arrow indicates the period of sub-freezing conditions. The “zero curtain” periods are also indicated.

Table 5 Number of Effective Freeze-Thaw Cycles (EFTCs) recorded by the Automatic Weather Station (AWS) and MicroTemp Dataloggers (MTs) in September, October and November 2016 and 2017. nd, no data.

MTs	EFTC 2016				EFTC 2017			
	Sept	Oct	Nov	Tot.	Sept	Oct	Nov	Tot.
AWS	0	5	8	13	3	5	8	16
1	0	2	5	7	1	1	7	9
2	0	4	0	4	2	2	0	4
3	0	9	2	11	3	3	2	8
4	0	10	2	12	1	1	1	3
5	0	4	0	4	0	0	1	1
6	nd	nd	nd	nd	1	0	1	2
7	nd	nd	nd	nd	1	1	13	15

4 Discussion

The identified rockfall events give an overview on the temporal and spatial distribution of the

process in the study area. Documented rockfalls range in volume from a few tens to several thousands of cubic meters. They concentrate in summer (as found also by [Luethi et al. 2015](#) for small-size rockfalls) and occurred mainly from NE and NW facing slopes characterized by permafrost in nearly all or mostly in cold conditions. In terms of seasonal distribution, inhomogeneities related to data reporting and acquisition timing exist. Considering the analysed data sources, aerial photos are usually taken at the end of the summer, when the snow cover is partially or totally absent: in these conditions it is quite difficult to identify rockfall deposits, because they often fall on pre-existing debris and cannot be easily distinguished, especially in case of small events. Moreover, summer events are generally more easily reported, due the higher mountain frequentation. Thus, events occurring in other seasons may be under- or no-represented ([Paranunzio et al. 2019](#)). The official landslide datasets (IFFI and SIFraP) and archives that were analysed provided some additional information on rockfall prone areas but not on dated events, probably because of the remoteness of the study area and because eventual instability events, luckily, did not affect people or human activities and infrastructures. Despite these information gaps we can: i) exclude that large events occurred in the area, because they would have been heard and reported from the inhabitants of the valley below, even in winter; ii) consider unlikely rockfall events in autumn, winter and spring because, despite a careful viewing of the webcam PANOMAX images during the entire operating period, we never saw any evidence of rockfall; in addition, the Gastaldi Hut opens also in spring and rockfall evidences would have been reported by the hut keeper.

The statistical analysis according to [Paranunzio et al. \(2019\)](#), performed for the dated events, revealed different behaviours. Although positive temperature anomalies (in other words, temperatures whose non-exceedance probability is above 90th percentile) have been detected in all analysed events, they occur at different temporal ranges and with different combination, linked to precipitation at times, like July events.

The two events occurred at the end of August (27 in 2017 and 23 in 2019) share a clear positive long-term temperature anomaly in three months

before the rockfalls. This could be contextualized into a generalized framework of global warming, since the first seven months of 2017 and 2019 turned out to be the warmest January-through-July periods on record ([NOAA 2020](#)), and confirmed at the local scale of the study area by our climatic analysis. In these two events, precipitation is not believed to have acted as preparatory or triggering factor, as recorded values are always below the 50th percentile. As already pointed out in previous studies, long-term (or wide-spread as in the August 2017 event) positive temperature anomaly could act a role in emphasizing permafrost thawing and thus in rock mass destabilization in depth ([Gruber and Haeberli 2007](#); [Ravanel et al. 2017](#)). Moreover, in August 2017, a combined effect of short and long-term temperature anomalies has been detected, with the former potentially enhancing the ongoing process of active-layer thickening in the days leading up to the event ([Gruber and Haeberli 2007](#); [Harris et al. 2009](#)).

July 2019 events showed significant positive temperature anomalies too but here, unlike events occurred in August 2019, a possible contribute of precipitation can be hypothesized, although values cannot be considered statistically significant, and a complex combination of factors has to be claimed responsible for failure initiation. In order to further investigate this point, snow height records from AWS have also been considered and analysed together with air temperature and precipitations for the period April-July 2019 ([Figure 8](#)). Here, air temperature has been translated at the detachment area elevation i.e., approximately 3000 m, through a linear lapse rate 0.65°C/100 m, and precipitation recorded by the AWS rain gauge has been distinguished into rainfall and snowfall (considering precipitation fallen with daily mean air temperature < 1°C) at the detachment zone.

The July 6 event occurred after a heatwave started in the second half of June, as confirmed by the positive temperature anomaly detected at monthly and weekly scales (see [Figure 6](#)). This long-lasting heatwave may have been responsible for the melting of the entire snow cover, as recorded by the AWS on 1st July ([Figure 8](#)). Positive temperatures allowed precipitations to fall as rain between 2nd and 4th July on a snow-free slope and water-saturated rock mass by the rapid

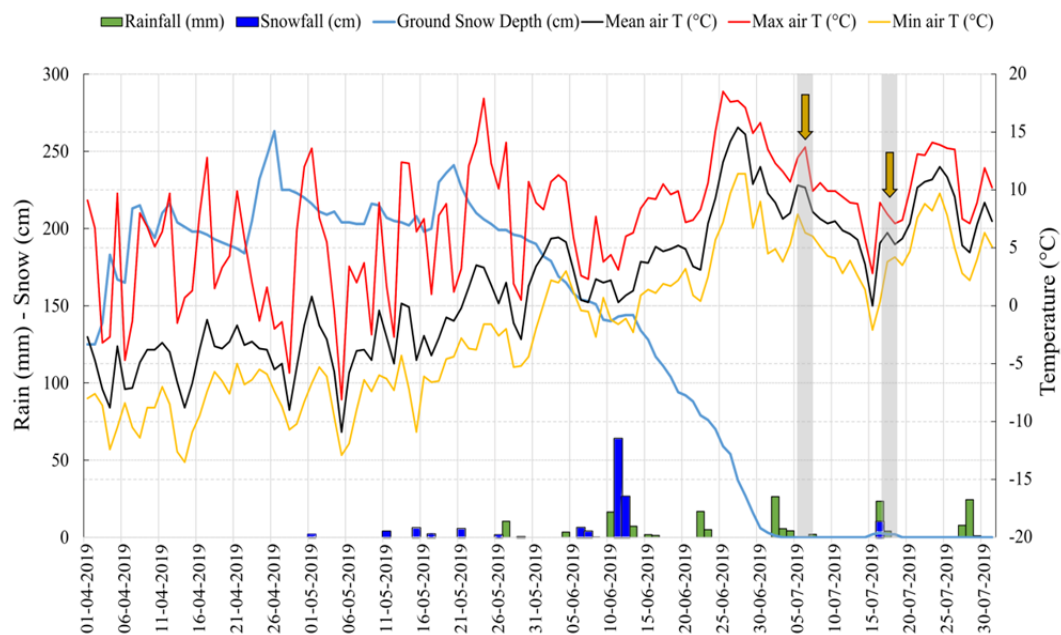


Figure 8 Ground snow depth (at AWS), air temperature (translated at the detachment height) and precipitation records (at AWS, but distinguished in rainfall and snowfall at the detachment zones, according to daily mean air temperature).

snow-melting (Dreabing et al. 2014). It is unclear if and how the sudden temperature rise occurred the day before the event (highlighted by temperature anomalies at the daily scale) might have enhanced the ongoing process.

The July 17 event may not have been occurred at the same time as the previous one because of the persisting snow cover on the terrace just above the rockfall-prone edge that could have prevented rainfall infiltration in the rock mass. Indeed, an image of the webcam dating September 7, 2017 clearly shows how the slope where the July 6, 2019 event occurred was completely snow-free, while the area where the July 17, 2019 event initiated was still snow-covered, because of the different topography. Rain-on-snow process due to the precipitation occurred on July 16, 2019 could have enhanced the ongoing snow-melting and increased water percolation through the rock: the rapid temperature increase on July 17 ($\Delta T_{\text{min-1}} = 0.96$) may have been the final trigger of the event, causing rapid melting of residual snow and water pressure increase inside the rock mass. Finally, for both the July events, monthly-scale temperature anomalies may have enhanced the seasonal thaw of the active layer.

Most of the rockfalls documented in this study occurred on NW to NE-facing slopes. Even though rock slopes in the study area have a prevailing N-

NE exposure, this aspect-dependent distribution of rockfalls is in agreement with the findings of other studies. In fact, some authors suggest that south-facing slopes exhibit diurnal freeze-thaw cycles all year long (Regmi and Watanabe 2009), as they are exposed to insolation-induced thermal stress and respond to changes in solar radiation faster than air temperature (Gruber et al. 2004b). Conversely, north-facing slopes are more susceptible to seasonal freeze-thaw cycles than south-west facing rock walls (Nagai et al. 2013). If on south-aspect walls snow-cover is variable and largely dependent on the solar radiation conditions, on north-facing slopes snow cover is generally long-lasting. Here, the length of the thawing period is generally shorter than on south-aspect slopes (Magnin et al. 2015) and the summer atmospheric warming is deemed to play a major role on thaw processes rather than solar radiation (Gruber et al. 2004b). This is well illustrated by the outcomes of our study. NSRT in sensors 2 and 4 drilled in rock faces with NE exposure (like many of the documented rockfall detachment zones) substantially follow air temperature pattern, independently by weather conditions (Figure 9); on the contrary, NSRT patterns recorded by sensors 3, 5 and 1 (facing E to W) are strictly dependent on solar radiation. This daily behaviour is reflected in annual NSRT vs air temperature values summarized in Table 4.

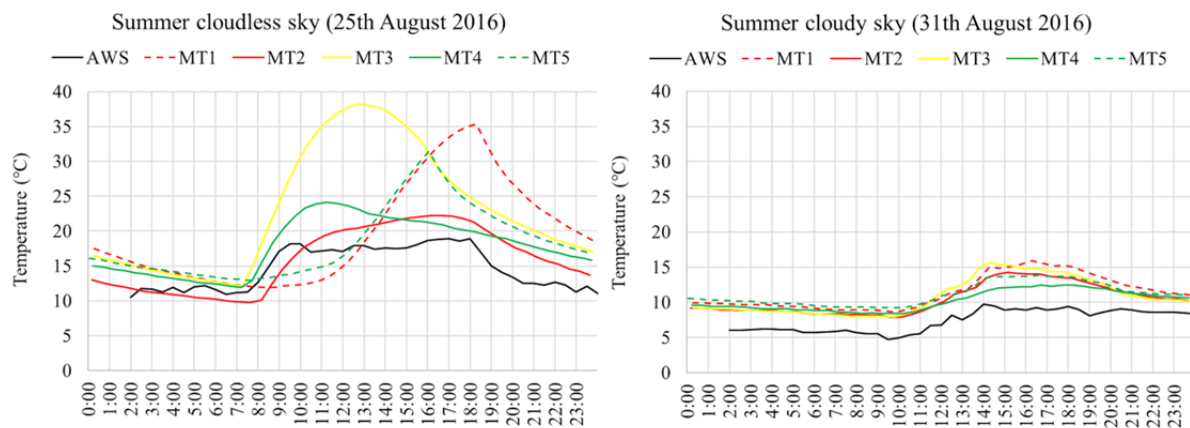


Figure 9 NSRT for MTs 1-5 and mean air temperature as recorded by AWS for two typical end-of-summer days with cloudless (August 25, 2016) and cloudy (August 31, 2016) sky.

Considering all this, distribution of documented rockfalls in the study area, both from a spatial point of view (on slopes exposed from NE to NW, in permafrost areas) and a temporal point of view (in summer, with an increasing frequency in recent years) would appear to be representative of the actual distribution of processes, and not only the result of incomplete information.

On the other hand, if we consider the outcomes of this study in the perspective of global climate warming, according to the number of icing days and summer air temperature trends in the study area, snow-melting is expected to be anticipated in time, making slopes which are not much exposed to solar radiation (like N-facing slopes), but affected by climate change effects anyway, more exposed to instability. We expect that climate change, by anticipating snow-melting and enhancing thawing of the active layer over time, could make these events occur on a wider time span during the year. Moreover, rising temperature trend will continue to impact on the Bessanese Glacier that already experienced a significant shrinkage in the last decades. Bessanese Glacier changes can be contextualized in the overall European glaciers evolution (Hock et al. 2019) which include a significant retreat of glacier fronts, the disappearing of the existing lobes and a general ice thickness loss (Salvatore et al. 2015). Two of the rockfall detachment areas identified in the present study (NE face of the Uja di Bessanese rock wall and SW slope of Punta Adami) are located nearby the glacier boundaries. Here, a rapid and significant (tens of meters) reduction of the glacier thickness surface occurred, thus triggering

debutressing phenomena (Kellerer-Pirklbauer et al. 2012; Grämiger et al. 2017). The progress of ice surface lowering might cause other parts of the slopes surrounding the glacier to become unstable, if their geological characteristics make them prone to failure. Finally, from a geomorphological point of view, the NE ridge of the Uja di Bessanese (where three of the documented events occurred) has a convex topography and the effects of the insolation are higher (Magnin et al. 2015). Gruber and Haeberli (2007) underlined that these kind of areas are subjected to rapid deep thaw due to warming from several sides, thus being preferred location of instability. In fact, several rockfall events in the European Alps started from similar area sources, such as Punta Tre Amici in the Monte Rosa massif (Chiarle et al. 2016), Arête des Cosmiques in the Mont Blanc chain (Ravanel et al. 2013) and Matterhorn (Chiarle et al. 2015).

5 Conclusion and Perspectives

Despite the numerous studies, much remains to be understood regarding the role of climatic factors in the preparation and triggering of slope failure at high altitudes, and therefore on the current and future effects of climate change on rockfall hazard. This is partly due to the complexity of climate-related processes that contribute to slope instability, and partly to the scarcity and spatio-temporal inhomogeneity of information.

With regard to the first criticality, the present study contributed with a cross-temporal analysis of the possible role of climate forcing in the preparation and initiation of the rockfalls

documented, for the last decades, in a glacierized basin of the Italian Alps. The main outcomes can be summarized as follows:

i) from a spatial point of view, rock falls occurred in two different geomorphological positions: along the glacier margins, on rock slopes uncovered by the ice in the last decades, and/or on rock slopes in permafrost condition, facing from NW to NE. Glacier debuitressing, rock weathering and/or seasonal thaw of the active layer can be claimed responsible for preparing slopes to failure.

ii) with regard to timing, almost all dated rock falls occurred during the summer. For the events occurred in July, we suggest that initiation may have been caused by a combination of rapid snow melt and enhanced seasonal thaw of the active layer due to anomalous warm temperatures, and rainfall. The events occurred in August are, instead, associated with a marked positive temperature anomaly on the quarterly scale, and they can, thus, be ascribed to the rapid and/or in depth thaw of the active layer of permafrost.

According to these interpretations, we can expect that in the Bessanese glacierized basin, as well as in similar high mountain areas, climate change has caused, and will further in the future, an increase of slope instability.

With regard to the scarcity and the spatio-temporal inhomogeneity of information, the present work proposes: i) a cross-temporal methodological approach that allows to interpret the most recent information coming from monitoring activities, in the broader context of the climatic and geomorphological evolution of the area; ii) an example of an “open-air” laboratory, specifically selected and equipped for the long-term study of the relationships between climate forcing and geomorphological dynamics, with a focus on slope instability, iii) the promotion, discussion and agreement on common procedures to establish measurement traceability and uncertainty analysis, to improve data comparability in time and space, among different networks and research groups.

Experimental sites like the one presented here are now active and managed by different research Institutions at European level and worldwide. To improve our understanding of the effects of climate change and associated risks, such installations should soon become part of a large network of

long-term instrumented sites, capable of representing a wide range of climatic and environmental conditions. At the same time, efforts must be dedicated to the development and adoption of standardized and shared monitoring strategies, to allow a real-time and effective comparison of the results.

Acknowledgments

This work was carried out in the framework of the RiST Project, co-financed by “Fondazione Cassa di Risparmio di Torino” and by MeteoMet Project. The authors wish to thank: Ing. Renato Riva (PANOMAX Italia) for setting up the visual monitoring of the basin; Ing. Secondo Barbero (ARPA Piemonte) for providing sensor data; Guido Rocci (Municipality of Balme) for the support given to the project; Roberto Chiosso (keeper of the Bartolomeo Gastaldi Hut) and his staff for the logistical support given to the project, and for documenting and reporting instability events in the experimental area; Giovanni Mortara and Stefano Perona (CGI) for providing and commenting historical documentation; Luigi Perotti for the expert advice on calculation with raster data; Paolo Silvestri and Davide Ricci (IRPI) for field data collection and for processing snow data series.

Author Contributions

Conceptualization: V.C., C.M., M.A., N.G.; methodology: V.C., C.M., M.A., N.G.; formal analysis: V.C., P.R., M.C., C.G., N.G.; investigation: V.C., P.R., M.C., N.G.; writing - original draft preparation: V.C., C.M., P.R., N.G.; writing - review and editing: V.C., C.M., P.R., M.A., M.C., C.G., N.G.; supervision: C.M., M.A., N.G.; project: N.G.; funding acquisition: N.G. All authors have read and agreed to the submitted version of the manuscript.

Open Access This article is distributed under the terms of the Creative Commons Attribution 4.0 International License

(<http://creativecommons.org/licenses/by/4.0/>), which permits unrestricted use, distribution, and reproduction in any medium, provided you give appropriate credit to the original author(s) and the source, provide a link to the Creative Commons license, and indicate if changes were made.

References

- Acquaotta F, Fratianni S, Garzena D (2015) Temperature changes in the North-Western Italian Alps from 1961 to 2010. Theoretical and Applied Climatology 122: 619–634.
<https://doi.org/10.1007/s00704-014-1316-7>
- Allen S, Huggel C (2013) Extremely warm temperatures as a potential cause of recent high mountain rockfall. Global and Planetary Change 107: 59–69.
<https://doi.org/10.1016/j.gloplacha.2013.04.007>
- Armando E, Baroni C, Meneghel M, et al. (2004) Reports of the glaciological survey 2003. Geografia Fisica e Dinamica Quaternaria 27(2): 167–225. (In Italian).
- Ballantyne CK (2002) Paraglacial geomorphology. Quaternary Science Reviews 21(18–19): 1935–2017.
[https://doi.org/10.1016/S0277-3791\(02\)00005-7](https://doi.org/10.1016/S0277-3791(02)00005-7)
- Baroni C, Bondesan A, Carturan L, et al. (2019) Annual glaciological survey of Italian glaciers 2018. Geografia Fisica e Dinamica Quaternaria 42(2): 113–202. (In Italian).
<https://doi.org/10.4461/GFDQ.2019.42.9>
- Barry R, Gan TY (2011) The Global Cryosphere. Past, Present and Future. Cambridge University Press, New York. 472 pp.
- Belotti P, Campus S, Cetti M, et al. (2013) DTMs in the Public Administration. In: Biagi L, Manzino AM, Sansò F (eds.), Bollettino della Società Italiana di Fotogrammetria e Topografia. Cagliari (IT), SIFET. pp 223–235. (In Italian).
- Boeckli L, Brenning A, Gruber S, et al. (2012) Permafrost distribution in the European Alps: calculation and evaluation of an index map and summary statistics. The Cryosphere 6: 807–820. <https://doi.org/10.5194/tc-6-807-2012>
- CGI (Comitato Glaciologico Italiano) (1959) Reports of the glaciological surveys 1956 and 1957. Bollettino del Comitato Glaciologico Italiano II(8): 1–185. (In Italian).
- CGI (Comitato Glaciologico Italiano) (1961) Reports of the glaciological surveys 1958 and 1959. Bollettino del Comitato Glaciologico Italiano II(9): 1–114. (In Italian).
- CGI (Comitato Glaciologico Italiano) (1996) Reports of the glaciological surveys 1995. Geografia Fisica e Dinamica Quaternaria 19: 147–198. (In Italian).
- CGI (Comitato Glaciologico Italiano) (2020) Annual Glaciological Surveys. <http://www.glaciologia.it/en/i-ghiacciai-italiani/le-campagne-glaciologiche/> (Accessed on 12 May 2020).
- CNR-CGI (Consiglio Nazionale delle Ricerche and Comitato Glaciologico Italiano) (1961) Inventory of Italian glaciers. International geophysical year 1957–1958. Glaciers of Piemonte region. Comitato Glaciologico Italiano, Torino (IT). pp 1–324. (In Italian).
- Chiarle M, Coviello V, Arattano M, et al. (2015) High elevation rock falls and their climatic control: a case study in the Conca di Cervinia (NW Italian Alps). In: Lollino G, Manconi A, Clague J, et al. (eds.), Engineering Geology for Society and Territory - Volume 1. Springer, Cham. pp 439–442.
https://doi.org/10.1007/978-3-319-09300-0_84
- Chiarle M, Mortara G, Tamburini A, et al. (2016) The 16th–17th december 2015 rockfall at Punta Tre Amici (Macugnaga, Monte Rosa). Nimbusweb, Torino (IT). (In Italian).
http://www.nimbus.it/ghiacciai/2016/160119_CrolloTreAmici.htm (Accessed on 12 May 2020).
- Collins B, Stock G (2016) Rockfall triggering by cyclic thermal stressing of exfoliation fractures. Nature Geoscience 9: 395–400.
<https://doi.org/10.1038/ngeo2686>
- D'Amato J, Hantz D, Guerin A, et al. (2016) Influence of meteorological factors on rockfall occurrence in a middle mountain limestone cliff. Natural Hazards and Earth System Sciences 16: 719–735. <https://doi.org/10.5194/nhess-16-719-2016>
- Deline P, Gruber S, Delaloye R, et al. (2015) Chapter 15 - Ice loss and slope stability in high-mountain regions. In: Shroder JF, Haeblerli W, Whiteman C (eds.), Snow and Ice-related hazards, risks and disasters. Academic Press. pp 521–561.
<https://doi.org/10.1016/B978-0-12-394849-6.00015-9>
- Di Matteo L, Romeo S, Kieffer DS (2017) Rock fall analysis in an Alpine area by using a reliable integrated monitoring system: results from the Ingelsberg slope (Salzburg Land, Austria). Bulletin of Engineering Geology and the Environment 76: 413–420. <https://doi.org/10.1007/s10064-016-0980-5>
- Draebing D, Haberkorn A, Krautblatter M, et al. (2017) Thermal and mechanical responses resulting from spatial and temporal snow cover variability in permafrost rock slopes, Steintaelli, Swiss Alps. Permafrost and Periglacial Processes 28(1): 140–157.
<https://doi.org/10.1002/ppp.1921>
- Draebing D, Krautblatter M (2019) The efficacy of frost weathering processes in alpine rockwalls. Geophysical Research Letters 46(12): 6516–6524. <https://doi.org/10.1029/2019GL081981>
- Draebing D, Krautblatter M, Dikau, R (2014) Interaction of thermal and mechanical processes in steep permafrost rock walls: A conceptual approach. Geomorphology 226: 226–235.
<https://doi.org/10.1016/j.geomorph.2014.08.009>
- Fischer L, Purves RS, Huggel C, et al. (2012) On the influence of topographic, geological and cryospheric factors on rock avalanches and rockfalls in high mountain areas. Natural Hazards and Earth System Science, 12: 241–254.
<https://doi.org/10.5194/nhess-12-241-2012>
- Gallach X, Ravello L, Egli M, et al. (2018) Timing of rockfalls in the Mont Blanc massif (Western Alps): evidence from surface exposure dating with cosmogenic ¹⁰Be. Landslides 15: 1991–2000.
<https://doi.org/10.1007/s10346-018-0999-8>
- Gariano SL, Guzzetti F (2016) Landslides in a changing climate. Earth-Science Reviews 162: 227–252.
<https://doi.org/10.1016/j.earscirev.2016.08.011>
- Grämiger LM, Moore JR, Gischig VS, et al. (2017) Beyond debulking: Mechanics of paraglacial rock slope damage during repeat glacial cycles. Journal of Geophysical Research: Earth Surface 122: 1004–1036.
<https://doi.org/10.1002/2016JF003967>
- Grämiger LM, Moore JR, Gischig VS, et al. (2018) Thermomechanical stresses drive damage of Alpine valley rock walls during repeat glacial cycles. Journal of Geophysical Research: Earth Surface 123: 2620–2646.
<https://doi.org/10.1029/2018JF004626>
- Gruber S, Haeblerli W (2007) Permafrost in steep bedrock slopes and its temperature-related destabilization following climate change. Journal of Geophysical Research 112: F02S18.
<https://doi.org/10.1029/2006JF000547>
- Gruber S, Hoelzle M, Haeblerli W (2004a) Permafrost thaw and destabilization of Alpine rock walls in the hot summer of 2003. Geophysical Research Letters 31: L13504.
<https://doi.org/10.1029/2004GL020051>
- Gruber S, Hoelzle M, Haeblerli W (2004b) Rock-wall temperature in the Alps: modelling their topographic distribution and regional differences. Permafrost and Periglacial Processes 15: 299–307.
<https://doi.org/10.1002/ppp.501>
- Guglielmin M, Worland MR, Baio F, et al. (2014) Permafrost and snow monitoring at Rothera Point (Adelaide Island, Maritime Antarctica): Implications for rock weathering in cryotic conditions. Geomorphology 225: 47–56.
<https://doi.org/10.1016/j.geomorph.2014.03.051>
- Haberkorn A, Phillips M, Kenner R, et al. (2015) Thermal regime of rock and its relation to snow cover in steep Alpine rock walls: gemsstock, central Swiss Alps. Geografiska Annaler: Series A, Physical Geography 97(3): 579–597.
<https://doi.org/10.1111/geoa.12101>
- Haeblerli W, Whiteman C (2015) Snow and Ice-related Hazards, Risks, and Disasters. A General Framework. In: Shroder JF, Haeblerli W, Whiteman C (eds.), Snow and Ice-related hazards, risks and disasters Academic Press. pp 1–34
<https://doi.org/10.1016/B978-0-12-394849-6.00001-9>
- Harris C, Arenson LU, Christiansen HH, et al. (2009) Permafrost and climate in Europe: Monitoring and modelling thermal, geomorphological and geotechnical responses. Earth-Science Reviews 92(3–4): 117–171.

- <https://doi.org/10.1016/j.earscirev.2008.12.002>
- Hasler A, Gruber S, Haeberli W (2011) Temperature variability and offset in steep alpine rock and ice faces. *The Cryosphere* 5: 977-988. <https://doi.org/10.5194/tc-5-977-2011>
- Hock R, Rasul G, Adler C, et al. (2019) High Mountain Areas. In: Pörtner HO, Roberts DC, Masson-Delmotte V, et al. (eds.), IPCC Special Report on the Ocean and Cryosphere in a Changing Climate 2: 131-202. https://www.ipcc.ch/site/assets/uploads/sites/3/2019/11/06_SROCC_Ch02_FINAL.pdf
- Huggel C, Clague JJ, Korup O (2012) Is climate change responsible for changing landslide activity in high mountains? *Earth Surface Processes and Landforms* 37(1): 77-91. <https://doi.org/10.1002/esp.2223>
- IFFI (Inventario dei Fenomeni Franosi in Italia) (2020) Italian Landslide Inventory (In Italian). <http://www.isprambiente.gov.it/it/progetti/suolo-e-territorio-1/iffi-inventario-dei-fenomeni-franosi-in-italia> (Accessed on 12 May 2020).
- Jia H, Xiang W, Krautblatter M (2015) Quantifying rock fatigue and decreasing compressive and tensile strength after repeated freeze - thaw cycles. *Permafrost and Periglacial processes* 26(4): 368-377. <https://doi.org/10.1002/ppp.1857>
- Kellerer P, Pirklbauer A, Lieb GK, Avian M, et al. (2012) Climate change and rock fall events in high mountain areas: Numerous and extensive rock falls in 2007 at Mittlerer Burgstall, Central Austria. *Geografiska Annaler: Series A, Physical Geography* 94(1): 59-78. <https://doi.org/10.1111/j.1468-0459.2011.00449.x>
- Krautblatter M, Funk D, Günzel FK (2013) Why permafrost rocks become unstable: a rock-ice - mechanical model in time and space. *Earth Surface Processes and Landforms* 38(8): 876-887. <https://doi.org/10.1002/esp.3374>
- Krautblatter M, Moser M. (2009) A nonlinear model coupling rockfall and rainfall intensity based on a four year measurement in a high Alpine rock wall (Reintal, German Alps). *Natural Hazards and Earth System Sciences* 9: 1425-1432. <https://doi.org/10.5194/nhess-9-1425-2009>
- Linsbauer A, Paul F, Haeberli W (2012) Modeling glacier thickness distribution and bed topography over entire mountain ranges with GlabTop: Application of a fast and robust approach. *Journal of Geophysical Research Earth Surface* 117: F03007. <https://doi.org/10.1029/2011JF002313>
- Lucchesi S, Fioraso G, Bertotto S, et al. (2014) Little Ice Age and contemporary glacier extent in the Western and South- Western Piedmont Alps (North-Western Italy). *Journal of Maps* 10(3): 409-423. <https://doi.org/10.1080/17445647.2014.880226>
- Luethi R, Gruber S, Ravel L (2015) Modelling transient ground surface temperatures of past rockfall events: Towards a better understanding of failure mechanisms in changing periglacial environments. *Geografiska Annaler: Series A, Physical Geography* 97(4): 753-767. <https://doi.org/10.1111/geoa.12114>
- Macciotta R, Martin CD, Cruden DM, et al. (2017) Rock fall hazard control along a section of railway based on quantified risk. *Georisk: Assessment and Management of Risk for Engineered Systems and Geohazards* 11(3): 272-284. <https://doi.org/10.1080/17499518.2017.1293273>
- Magnin F, Deline P, Ravel L, et al. (2015) Thermal characteristics of permafrost in the steep alpine rock walls of the Aiguille du Midi (Mont Blanc Massif, 3842 m asl). *The Cryosphere* 9: 109-121. <https://doi.org/10.5194/tc-9-109-2015>
- Magnin F, Josnin JY, Ravel L, et al. (2017) Modelling rock wall permafrost degradation in the Mont Blanc massif from the LIA to the end of the 21st century. *The Cryosphere* 11: 1813-1834. <https://doi.org/10.5194/tc-11-1813-2017>
- Mair V, Zischg A, Lang K, et al. (2011) PermaNET - Permafrost Long-term Monitoring Network. Synthesis report. INTERPRAEVENT Journal series 1, Report 3. Klagenfurt. 28 pp.
- Mamot P, Weber S, Schröder T, et al. (2018) A temperature-and stress-controlled failure criterion for ice-filled permafrost rock joints. *The Cryosphere* 12: 3333-3353. <https://doi.org/10.5194/tc-12-3333-2018>
- Matasci B, Stock GM, Jaboyedoff M, et al. (2018) Assessing rockfall susceptibility in steep and overhanging slopes using three-dimensional analysis of failure mechanisms. *Landslides* 15: 859-878. <https://doi.org/10.1007/s10346-017-0911-y>
- Matsuoka N (1990) The rate of rock weathering by frost action: Field measurements and predictive model. *Earth Surface Processes and Landforms* 15(1): 73-90. <https://doi.org/10.1002/esp.3290150108>
- Matsuoka N (2019) A multi-method monitoring of timing, magnitude and origin of rockfall activity in the Japanese Alps. *Geomorphology* 336: 65-76. <https://doi.org/10.1016/j.geomorph.2019.03.023>
- Matsuoka N, Hirakawa K, Watanabe T, et al. (1998) The role of diurnal, annual and millennial freeze-thaw cycles in controlling alpine slope instability. In: Proceedings of the Seventh International Conference on Permafrost. Centre d'etudes nordiques, Université Laval. pp 711-717.
- McColl ST, Davies TRH (2012). Large ice-contact slope movements; glacial buttressing, deformation and erosion. *Earth Surface Processes and Landforms* 38(10): 1102-1115. <https://doi.org/10.1002/esp.3346>
- McColl ST, Draebing D (2019) Rock slope instability in the proglacial zone: State of the Art. In: Heckmann T, Morche D (eds.), *Geomorphology of Proglacial Systems. Geography of the Physical Environment*. Springer, Cham. pp 119-141. https://doi.org/10.1007/978-3-319-94184-4_8
- Merlone A, Lopardo G, Sanna F, et al. (2015) The MeteoMet project - metrology for meteorology: challenges and results. *Meteorological Applications* 22(S1): 820-829. <https://doi.org/10.1002/met.1528>
- Merlone A, Sanna F, Beges G, et al. (2018) The MeteoMet2 project - highlights and results. *Measurement Science and Technology* 29 (2): 025802. <https://doi.org/10.1088/1361-6501/aa99fc>
- Messenzehl K, Meyer H, Otto JC, et al. (2017) Regional-scale controls on the spatial activity of rockfalls (Turtmann Valley, Swiss Alps) - A multivariate modeling approach. *Geomorphology* 287: 29-45. <https://doi.org/10.1016/j.geomorph.2016.01.008>
- Mourey J, Marcuzzi M, Ravel L, et al. (2019) Effects of climate change on high Alpine mountain environments: Evolution of mountaineering routes in the Mont Blanc massif (Western Alps) over half a century. *Arctic, Antarctic, and Alpine Research* 51(1): 176-189. <https://doi.org/10.1080/15230430.2019.1612216>
- Nagai H, Fujita K, Nuimura T, et al. (2013) Southwest-facing slopes control the formation of debris-covered glaciers in the Bhutan Himalaya. *The Cryosphere* 7: 1303-1314. <https://doi.org/10.5194/tc-7-1303-2013>
- Nigrelli G, Chiarle M, Merlone A, et al. (2018c) Rock and debris temperature in the alpine cryosphere. *PANGAEA* <https://doi.pangaea.de/10.1594/PANGAEA.894317>
- Nigrelli G, Chiarle M, Silvestri P, et al. (2018b) Rock-face temperature at high-elevation sites. A new measuring approach. Book of abstracts of the 5th European Conference on Permafrost, EUCOP, Chamonix, 23th June - 1st July. 527-528. <https://hal.archives-ouvertes.fr/hal-01816115v2/document>
- Nigrelli G, Fratianni S, Zampollo A, et al. (2018a) The altitudinal temperature lapse rates applied to high elevation rockfalls studies in the Western European Alps. *Theoretical and Applied Climatology* 131: 1479-1491. <https://doi.org/10.1007/s00704-017-2066-0>
- Nigrelli G, Lucchesi S, Bertotto S, et al. (2015) Climate variability and Alpine glaciers evolution in Northwestern Italy from the Little Ice Age to the 2010s. *Theoretical and Applied Climatology* 122: 595-608. <https://doi.org/10.1007/s00704-014-1313-x>
- Nimbus (2015) Ciardoney Glacier: mass losses and ice thickness evaluation by georadar measurements (In Italian) http://www.nimbus.it/ghiacciai/2015/150918_Ciardoney.htm (Accessed on 12 May 2020).
- NOAA (National Centers for Environmental Information) (2020) State of the Climate: Global Climate Report for Annual 2019. <https://www.ncdc.noaa.gov/sotc/global/201913> (Accessed on 12 May 2020).
- Occhiena C, Coviello V, Arattano M, et al. (2012) Analysis of microseismic signals and temperature recordings for rock slope

- stability investigations in high mountain areas. *Natural Hazards and Earth System Sciences* 12: 2283–2298. <https://doi.org/10.5194/nhess-12-2283-2012>
- Orombelli G (2011) Holocene mountain glacier fluctuations: a global overview. *Geografia Fisica e Dinamica Quaternaria* 34 (1): 17–24. <https://doi.org/10.4461/GFDQ.2011.34.2>
- Paranunzio R, Chiarle M, Laio F, et al. (2019) New insights in the relation between climate and slope failures at high-elevation sites. *Theoretical and Applied Climatology* 137: 1765–1784. <https://doi.org/10.1007/s00704-018-2673-4>
- Paranunzio R, Laio F, Chiarle M, et al. (2016) Climate anomalies associated with the occurrence of rockfalls at high-elevation in the Italian Alps. *Natural Hazards and Earth System Sciences* 16: 2085–2106. <https://doi.org/10.5194/nhess-16-2085-2016>
- Patton AI, Rathburn SL, Capps DM (2019) Landslide response to climate change in permafrost regions. *Geomorphology* 340: 116–128. <https://doi.org/10.1016/j.geomorph.2019.04.029>
- Peel MC, Finlayson BL, McMahon TA (2007) Updated world map of the Köppen-Geiger climate classification. *Hydrology and Earth System Sciences* 11: 1633–1644. <https://doi.org/10.5194/hess-11-1633-2007>
- Phillips M, Haberkorn A, Draebing D, et al. (2016) Seasonally intermittent water flow through deep fractures in an Alpine Rock Ridge: Gemsstock, Central Swiss Alps. *Cold Regions Science and Technology* 125: 117–127. <https://doi.org/10.1016/j.coldregions.2016.02.010>
- Phillips M, Wolter A, Lüthi R, et al. (2017) Rock slope failure in a recently deglaciated permafrost rock wall at Piz Kesch (Eastern Swiss Alps), February 2014. *Earth Surface Processes and Landforms* 42(3): 426–438. <https://doi.org/10.1002/esp.3992>
- Piana F, Fioraso G, Irace A, et al. (2017) Geology of Piemonte region (NW Italy, Alps-Apennines interference zone). *Journal of Maps* 13(2): 395–405. <https://doi.org/10.1080/17445647.2017.1316218>
- Pratt C, Macciotta R, Hendry M (2019) Quantitative relationship between weather seasonality and rock fall occurrences north of Hope, BC, Canada. *Bulletin of Engineering Geology and the Environment* 78: 3239–3251. <https://doi.org/10.1007/s10064-018-1358-7>
- Purdie H, Gomez C, Espiner S (2011) Glacier recession and the changing rockfall hazard: Implications for glacier tourism. *New Zealand Geographer* 71(3): 189–202. <https://doi.org/10.1111/nzg.12091>
- Raveland L, Deline P (2011) Climate influence on rockfalls in high-Alpine steep rockwalls: The north side of the Aiguilles de Chamonix (Mont Blanc massif) since the end of the ‘Little Ice Age’. *The Holocene* 21(2): 357–365. <https://doi.org/10.1177/0959683610374887>
- Raveland L, Deline P, Lambiel C, et al. (2013) Instability of a high alpine rock ridge: the lower arête des Cosmiques, Mont Blanc massif, France. *Geografiska Annaler: Serier A, Physical Geography* 95(1): 51–66. <https://doi.org/10.1111/geoa.12000>
- Raveland L, Magnin F, Deline P (2017) Impacts of the 2003 and 2015 summer heatwaves on permafrost-affected rock-walls in the Mont Blanc massif. *Science of the Total Environment* 609: 132–143. <https://doi.org/10.1016/j.scitotenv.2017.07.055>
- Raveland L, Magnin F, Duvillard PA, et al. (2018) Contribution of the PrévRisk Haute Montagne project to knowledge and management of risks related to alpine permafrost. 5th European Conference On Permafrost, Jun 2018, Chamonix, France.
- Regmi D, Watanabe T (2009) Rockfall activity in the Kangchenjunga area, Nepal Himalaya. *Permafrost and Periglacial Processes* 20: 390–398. <https://doi.org/10.1002/ppp.664>
- Salvatore MC, Zanoner T, Baroni C, et al. (2015) The state of Italian glaciers: a snapshot of the 2006–2007 hydrological period. *Geografia Fisica e Dinamica Quaternaria* 38(2): 175–198. <https://doi.org/10.4461/GFDQ.2015.38.16>
- Sass O (2005) Rock moisture measurements: techniques, results, and implications for weathering. *Earth Surface Processes and Landforms* 30(3): 359–374. <https://doi.org/10.1002/esp.1214>
- Schlögel R, Kofler C, Gariano SL, et al. (2020) Changes in climate patterns and their association to natural hazard distribution in South Tyrol (Eastern Italian Alps). *Scientific Reports* 10: 5022. <https://doi.org/10.1038/s41598-020-61615-w>
- SIFRaP (Sistema Informativo dei Fenomeni Franosì) (2017) Landslide Information System of Piemonte Region (In Italian). Agenzia Regionale per la Protezione dell’Ambiente, Torino (I). <http://www.arpa.piemonte.it/approfondimenti/temi-ambientali/geologia-e-dissesto/bancadatiged/sifrap> (Accessed on 12 May 2020).
- Smiraglia C, Azzoni RS, D’agata C, et al. (2015) The evolution of the Italian glaciers from the previous data base to the New Italian Inventory. Preliminary considerations and results. *Geografia Fisica e Dinamica Quaternaria* 38(1): 79–87. <https://doi.org/10.4461/GFDQ.2015.38.08>
- Sneyers R (1990) On the statistical analysis of series of observations. World Meteorological Organization, Technical Note N° 143, WMO-N° 415, Geneva. 218 pp.
- Štěpánek P (2006) AnClim - software for time series analysis. Department of Geography, Faculty of Natural Sciences, MU, Brno, 1.47 MB. <http://www.climahom.eu/software-solution/anclim> (Accessed on 12 May 2020).
- Stoffel M, Lièvre I, Monbaron M, et al. (2005) Seasonal timing of rockfall activity on a forested slope at Täschgufer (Swiss Alps) - a dendrochronological approach. *Zeitschrift für Geomorphologie* 49(1): 89–106.
- Thapa P, Martin YE, Johnson EA (2017) Quantification of controls on regional rockfall activity and talus deposition, Kananaskis, Canadian Rockies. *Geomorphology* 299: 107–123. <https://doi.org/10.1016/j.geomorph.2017.09.039>
- Vehling L, Rohn J, Moser M (2016) Quantification of small magnitude rockfall processes at a proglacial high mountain site, Gepatsch glacier (Tyrol, Austria). *Zeitschrift für Geomorphologie* 60(1): 93–108. https://doi.org/10.1127/zfg_suppl/2015/S-00184
- Viani C, Giardino M, Huggel C, et al. (2016) An overview of glacier lakes in the Western Italian Alps from 1927 to 2014 based on multiple data sources (historical maps, orthophotos and reports of the glaciological surveys). *Geografia Fisica e Dinamica Quaternaria* 39(2): 203–214. <https://doi.org/10.4461/GFDQ.2016.39.19>
- Viani C, Machguth H, Huggel C, et al. (2020) Potential future lakes from continued glacier shrinkage in the Aosta Valley Region (Western Alps, Italy). *Geomorphology* 355: 107068. <https://doi.org/10.1016/j.geomorph.2020.107068>
- Wang D, Kääb A (2015) Modeling glacier elevation change from DEM time series. *Remote Sensing* 7(8): 10117–10142. <https://doi.org/10.3390/rs70810117>
- Weber S, Beutel J, Faillietaz J, et al. (2017) Quantifying irreversible movement in steep, fractured bedrock permafrost on Matterhorn (CH). *The Cryosphere* 11: 567–583. <https://doi.org/10.5194/tc-11-567-2017>
- WMO (World Meteorological Organization) (2009) Guidelines on analysis of extremes in a changing climate in support of informed decisions for adaptation. WMO-TD No. 1500. Geneva (CH). 55 pp.
- Zangerl C, Fey C, Prager C (2019) Deformation characteristics and multi-slab formation of a deep-seated rock slide in a high alpine environment (Bliggspitze, Austria). *Bulletin of Engineering Geology and the Environment* 78: 6111–6130. <https://doi.org/10.1007/s10064-019-01516-z>
- Zhang T (2005) Influence of the seasonal snow cover on the ground thermal regime: An overview. *Reviews of Geophysics* 43: RG4002. <https://doi.org/10.1029/2004RG000157>